

# Quintessential Implications of the presence of AdS in the Dark Energy sector

Purba Mukherjee,<sup>1,\*</sup> Dharmendra Kumar,<sup>2,†</sup> and Anjan A Sen<sup>1,‡</sup>

<sup>1</sup>Centre for Theoretical Physics, Jamia Millia Islamia, New Delhi-110025, India

<sup>2</sup>Malaviya National Institute Of Technology Jaipur-302017, Rajasthan, India

(Dated: January 31, 2025)

We explore the implications of incorporating an Anti-de Sitter (AdS) vacua in the Dark Energy (DE) sector using the recent DESI BAO measurements in combination with Planck-2018 CMB, Pantheon-Plus(+SH0ES) supernovae and KiDS weak lensing data. We show that the presence of a *Negative Cosmological Constant* ( $\Lambda < 0$ , nCC) together with an evolving part (modelled by the CPL parametrisation) in DE sector allows a *non-phantom* region for the DE in the constrained parameter space consistent with different observational data. This essentially solves the problem of *phantom* behaviour in the DE sector which is difficult to obtain through reasonable field theory. The implications nCC in the DE sector for different cosmological tensions are also studied. Our findings highlight the importance of the presence of AdS in the DE sector for theoretical model building, especially in the context of quantum gravity theories, e.g. string theory.

Over the past few decades, cosmology has made significant progress, largely due to precise observations from the Cosmic Microwave Background (CMB) [1, 2], Type Ia supernovae (SN-Ia) [3–5], large-scale structure (LSS) and galaxy surveys [6–9]. These have improved our understanding of the universe’s composition, expansion, and structure. The standard model of cosmology,  $\Lambda$ CDM, suggests that the universe is primarily made up of cold dark matter (CDM) and dark energy (DE), described by a positive cosmological constant [10]( $\Lambda$ ) responsible for the universe’s accelerated expansion [11, 12]. However, recent observations have revealed some key issues [13–15], such as the Hubble tension [16] ( $> 5\sigma$  disagreement between local measurements of the Hubble constant  $H_0$  and CMB-based estimates), and the  $\sigma_8$  tension [17] ( $\approx 2.5\sigma$  mismatch between the CMB-predicted and observed clustering of matter from galaxy surveys [18–20]). Furthermore, deep-space James Webb Space Telescope (JWST) observations have identified the existence of massive and bright galaxies at redshifts  $z \gtrsim 7$  [21, 22], which is difficult to obtain with standard  $\Lambda$ CDM model. These discrepancies point to potential gaps in our understanding of the universe’s expansion and structure formation, suggesting the need for modifications to the 6-parameter baseline  $\Lambda$ CDM framework [23–25]

The nature of dark energy remains one of the biggest challenges in cosmology [26, 27]. Recent baryon acoustic oscillation (BAO) data from the Dark Energy Spectroscopic Instrument (DESI) suggest that the DE equation of state(EoS) may evolve with cosmic time, with indications of early phantom-like behaviour [28, 29]. While the DESI data are consistent with the  $\Lambda$ CDM model, extending the model to CPLCDM shows deviations from  $w = -1$ . Combining these observations with CMB and Pantheon-Plus SN-Ia data, the CPLCDM model provides a better fit, excluding  $\Lambda$ CDM at  $> 2.5\sigma$  confidence level (CL). The data suggest a preference for an early-phantom to late-non-phantom transition in the DE EoS, prompting the community to search for alternative scenarios for

explaining the cosmic dark sector [30–48].

In this context, the idea of a *negative cosmological constant* (nCC), described by  $\Lambda < 0$ , which can naturally be realized in an anti-de Sitter (AdS) vacuum, has gained interest[49, 50]. Although constructing de Sitter (dS) vacua in string theory is challenging [51–55], AdS vacua can be more easily realized within the string landscape [56]. Recent studies have shown that AdS vacua might help address the cosmological tensions and discrepancies observed in the CMB, BAO, and even JWST data [57–68]. While a nCC alone cannot drive the universe’s accelerated expansion, it could coexist with a positive DE component, providing a potential framework for understanding the nature of dark energy.

In this *letter*, we investigate the implications of AdS vacua in the DE sector in light of recent cosmological observations. Our findings demonstrate that there exists a finite non-phantom region in the  $w_0 - w_a$  space parameter when the evolving DE fluid is described by the CPL parametrization [69, 70]. This allows for the DE to be only non-phantom at all times, within the  $2\sigma$  CL, suggesting that scalar field theories can effectively model DE evolution without violating the null energy condition (NEC) [71, 72]. We also discuss the possibility of resolving the current cosmological tensions - mainly  $H_0$  and  $S_8$  tensions - in DE models with nCC.

We outline the cosmological framework for a spatially flat Friedmann-Lemaître-Robertson-Walker (FLRW) universe, where the Hubble parameter is

$$H^2(z) = H_0^2 [\Omega_m(1+z)^3 + \Omega_r(1+z)^4 + \Omega_{DE}(z)] . \quad (1)$$

Here  $z$  is the redshift,  $H_0$  is the Hubble parameter and  $\Omega_i$  are the density parameters at the present epoch. We assume the presence of nCC ( $\Lambda < 0$ ) in the DE sector, i.e. total DE density,  $\rho_{DE} = \rho_\phi + \Lambda$ .  $\rho_\phi$  is the evolving part of DE which in principle can be modeled by a minimally coupled slow-rolling scalar field [71, 72].  $\rho_{DE}$  must remain positive in the late time to drive the acceleration

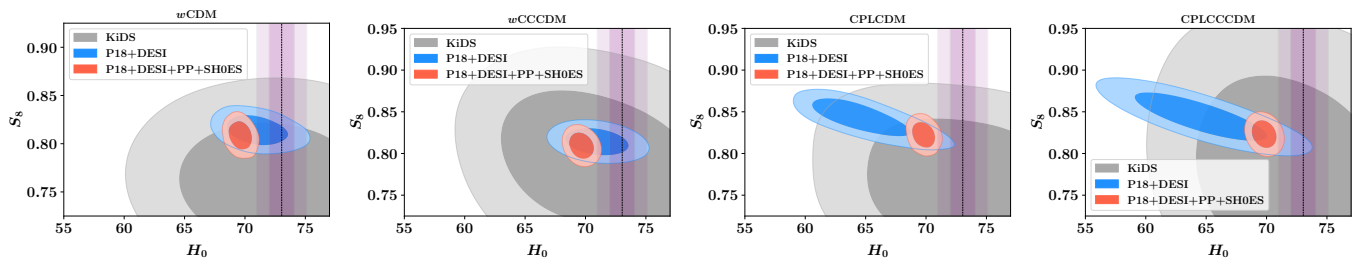


FIG. 1: 2D confidence contours at 68% and 95% confidence levels for  $H_0$  and  $S_8$ , as inferred using the four models:  $w\text{CDM}$ ,  $w\text{CCCDM}$ ,  $\text{CPLCDM}$ , and  $\text{CPLCCCDM}$ . The contours are derived from the different dataset combinations listed in the legends. The purple band represents the  $H_0$  measurement by the SH0ES collaboration.

of the universe. With this, the density parameter of DE is expressed as

$$\Omega_{\text{DE}}(z) = \Omega_\phi f(z) + \Omega_\Lambda, \quad (2)$$

where  $f(z)$  captures the evolution of the scalar field, is defined as  $f(z) = \exp\left[3 \int_0^z \frac{1+w_\phi(z')}{1+z'} dz'\right]$ . The flatness condition requires  $\Omega_m + \Omega_r + \Omega_\phi + \Omega_\Lambda = 1$ . At present, the combined DE sector satisfies,

$$\Omega_{\text{DE}}(z=0) = \Omega_\Lambda + \Omega_\phi \approx 1 - \Omega_m - \Omega_r. \quad (3)$$

Without specifying the potential  $V(\phi)$  for the scalar field, we adopt two parametrizations for  $w_\phi = p_\phi/\rho_\phi$  viz. (i)  $w_\phi = w_0$  (constant), (ii)  $w_\phi = w_0 + w_a \left(\frac{z}{1+z}\right)$  (i.e., CPL parametrization [69, 70]). These models correspond to the  $w\text{CCCDM}$  and  $\text{CPLCCCDM}$  frameworks, which we compare against the conventional  $w\text{CDM}$  and  $\text{CPLCDM}$  models with  $\Lambda = 0$ . We aim to study whether the nCC brings new signatures in the DE sector. Additionally, we seek to explore if it can convincingly address the  $H_0$  and  $S_8$  tensions and provide new insights into cosmic evolution.

We use the following datasets in our analysis:

- **P18**: The full Planck-PR3 CMB likelihood [1] (2018), including high- $l$  Plik for TT, TE, and EE spectra, low- $l$  commander for TT, low- $l$  SimAll for EE spectra, and Plik lensing measurements derived from the temperature 4-point correlation function.
- **DESI**: 12 DESI-BAO DR1 [28] measurements across the redshift range  $0.1 < z < 4.2$ , including volume-averaged distance  $D_V(z)/r_d$ , angular diameter distance  $D_M(z)/r_d$ , and comoving Hubble distance  $D_H(z)/r_d$ , where  $r_d$  is the sound horizon at the drag epoch.
- **PP**: The Pantheon Plus [3] SN-Ia compilation, consisting of 1701 light curves from 1550 distinct SN-Ia in the redshift range  $0.01 < z < 2.26$ . When incorporating SH0ES [15] Cepheid host distances as calibrators, this dataset is referred to as **PP+SH0ES**.
- **KiDS**: Weak lensing (WL) data from the KiDS-1000 [73] survey, analyzed using COSEBIs [74] to separate E-mode and B-mode contributions.

The numerical analysis is conducted using the Boltzmann solver CLASS [75], with parameter constraints derived via MCMC from MontePython [76, 77] and Cobaya [78], assuming uniform flat priors on the model parameters  $\{\Omega_b h^2, \Omega_c h^2, \tau, n_s, \log[10^{10} A_s], 100 \theta_*, w_0, w_a, \Omega_\phi\}$ . A Gelman-Rubin convergence criterion of  $R-1 < 0.02$  ensures the convergence of the chains. Results are visualized using GetDist [79], and Bayesian evidence is computed using MultiNest [80, 81].

We summarize the constraints on cosmological parameters at 68% confidence levels in Tab. I. The most important findings are as follows:

1. The constraints on  $H_0$  for all four models, both with and without the inclusion of nCC, show that the  $H_0$  values are similar across the models, regardless of the data set used. Adding an extra parameter,  $\Omega_\Lambda$ , to account for the nCC in the dark energy sector results in slightly relaxed confidence intervals compared to models where  $\Omega_\Lambda = 0$ . This relaxation helps address the  $H_0$  tension more effectively, without causing significant shifts in the mean values. Importantly, there is no deterioration in the parameter constraints for the nCC models as far as the mean values are concerned.
2. For  $S_8$ , the KiDS data suggests that models with nCC contributions tend to favour higher  $S_8$  values, which are closer to the Planck CMB measurements when compared to their non-nCC i.e.,  $\Omega_\Lambda = 0$  counterparts. This demonstrates that nCC models can better alleviate the  $S_8$  tension with WL data. However, for the P18+DESI and P18+DESI+PP (CMB-anchored  $S_8$ ), there is no noticeable difference between the models with or without nCC contributions.
3. Fig. 1 showcases the 2D contour plots for the  $H_0 - S_8$  parameter space across the four models. For the P18+DESI combination, the data comfortably accommodates the SH0ES  $H_0 = 73.04 \pm 1.04 \text{ km Mpc}^{-1} \text{ s}^{-1}$  measurement [15] within  $2\sigma$  confidence level. So, we

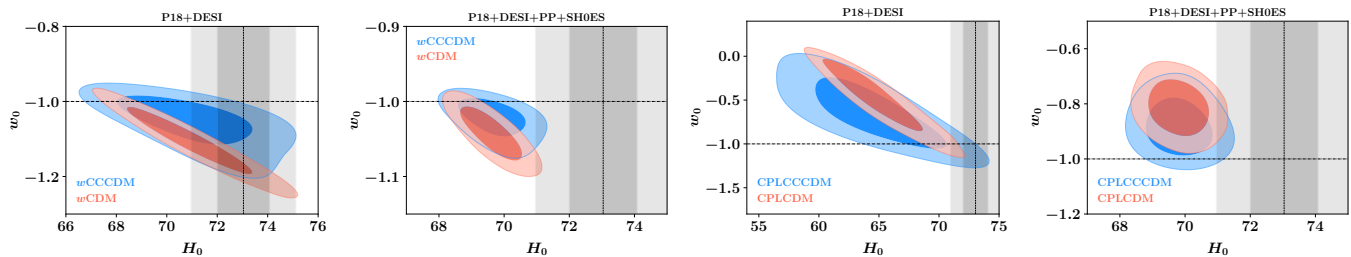


FIG. 2: 2D confidence contours at 68% and 95% confidence levels for  $H_0$  and  $w_0$ , illustrating the impact of including nCC by comparing  $w$ CDM with  $w$ CCCDM and CPLCDM with CPLCCCDM for two dataset combinations: P18+DESI and P18+DESI+PP+SH0ES respectively.

KiDS				
Parameter	$w$ CDM	$w$ CCCDM	CPLCDM	CPLCCCDM
$\Omega_m$	$0.278^{+0.073}_{-0.099}$	$0.288^{+0.059}_{-0.099}$	$0.263^{+0.059}_{-0.084}$	$0.291^{+0.087}_{-0.10}$
$w_0$	$-0.98^{+0.36}_{-0.22}$	$-0.88 \pm 0.17$	$-0.93^{+0.59}_{-0.17}$	$-0.79^{+0.40}_{-0.25}$
$w_a$	-	-	$-0.60^{+0.92}_{-0.68}$	$-1.2^{+1.1}_{-1.0}$
$\Omega_\Lambda$	0	$-1.50^{+0.63}_{-0.38}$	0	$-1.4^{+1.6}_{-2.3}$
$H_0$	$72.8^{+4.7}_{-5.2}$	$71.2^{+3.7}_{-6.1}$	$73.5 \pm 5.2$	$72.7^{+4.9}_{-6.1}$
$S_8$	$0.756^{+0.038}_{-0.042}$	$0.792^{+0.050}_{-0.045}$	$0.760 \pm 0.053$	$0.774^{+0.079}_{-0.088}$
P18+DESI				
Parameter	$w$ CDM	$w$ CCCDM	CPLCDM	CPLCCCDM
$\Omega_m$	$0.283 \pm 0.013$	$0.283 \pm 0.013$	$0.342^{+0.032}_{-0.027}$	$0.345^{+0.033}_{-0.040}$
$w_0$	$-1.108^{+0.064}_{-0.054}$	$-1.052^{+0.048}_{-0.016}$	$-0.47^{+0.32}_{-0.22}$	$-0.65^{+0.19}_{-0.29}$
$w_a$	-	-	$-1.71^{+0.59}_{-0.92}$	$-1.09^{+0.86}_{-0.49}$
$\Omega_\Lambda$	0	$-1.14^{+1.2}_{-0.38}$	0	$-0.63^{+0.70}_{-0.10}$
$H_0$	$71.0^{+1.5}_{-1.8}$	$70.9^{+1.5}_{-1.7}$	$64.8^{+2.1}_{-3.2}$	$64.6^{+3.2}_{-3.6}$
$S_8$	$0.814 \pm 0.010$	$0.814 \pm 0.010$	$0.842^{+0.017}_{-0.013}$	$0.844 \pm 0.018$
P18+DESI+PP				
Parameter	$w$ CDM	$w$ CCCDM	CPLCDM	CPLCCCDM
$\Omega_m$	$0.3087 \pm 0.0068$	$0.3088 \pm 0.0069$	$0.3079 \pm 0.0068$	$0.3081 \pm 0.0069$
$w_0$	$-0.990 \pm 0.026$	$-0.9952^{+0.0097}_{-0.012}$	$-0.834 \pm 0.064$	$-0.894^{+0.038}_{-0.073}$
$w_a$	-	-	$-0.71^{+0.29}_{-0.26}$	$-0.44^{+0.32}_{-0.15}$
$\Omega_\Lambda$	0	$-1.30^{+1.4}_{-0.47}$	0	$-0.66^{+0.75}_{-0.10}$
$H_0$	$67.74 \pm 0.70$	$67.72 \pm 0.71$	$68.04 \pm 0.71$	$68.03 \pm 0.73$
$S_8$	$0.817 \pm 0.010$	$0.817 \pm 0.010$	$0.827 \pm 0.011$	$0.827 \pm 0.011$
P18+DESI+PP+SH0ES				
Parameter	$w$ CDM	$w$ CCCDM	CPLCDM	CPLCCCDM
$\Omega_m$	$0.2915 \pm 0.0056$	$0.2913 \pm 0.0056$	$0.2927 \pm 0.0056$	$0.2928 \pm 0.0057$
$w_0$	$-1.043 \pm 0.024$	$-1.022^{+0.019}_{-0.0076}$	$-0.814 \pm 0.068$	$-0.883^{+0.041}_{-0.082}$
$w_a$	-	-	$-1.05 \pm 0.31$	$-0.65^{+0.43}_{-0.21}$
$\Omega_\Lambda$	0	$-1.21^{+1.3}_{-0.44}$	0	$-0.59^{+0.70}_{-0.11}$
$H_0$	$69.62 \pm 0.62$	$69.67 \pm 0.63$	$69.80 \pm 0.61$	$69.81 \pm 0.63$
$S_8$	$0.8085 \pm 0.0098$	$0.8094 \pm 0.0097$	$0.822 \pm 0.010$	$0.823 \pm 0.010$

TABLE I: Constraints at 68% confidence levels on the cosmological model parameters for different data combinations

can include the SH0ES Cepheid calibration for the PP SN-Ia data, leading to the P18+DESI+PP+SH0ES data combination. In nCC models, the  $H_0 - S_8$  parameter space shows significant overlap within the  $1\sigma$  region only, whereas, for non-nCC counterparts, the overlap extends also to the  $2\sigma$  region.

4. In the  $H_0 - w_0$  parameter space, the inclusion of nCC in the dark energy sector results in slightly broader confidence intervals, as shown in Fig. 2. With nCC

models, the combination of P18 + DESI can accommodate the higher  $H_0$  value from the SH0ES Collaboration [15] consistently within  $1\sigma$  CL, without significant deviation from  $w_0 = -1$ . When PP+SH0ES data is added to P18 + DESI, the nCC models display a  $2\sigma$  overlap region with the SH0ES  $H_0$  value, which is slightly larger compared to their non-nCC counterparts. With the P18+DESI+PP+SH0ES data, only for the CPLCCCDM model, the region of the  $H_0 - w_0$  parameters space that is consistent with SH0ES  $H_0$  include  $w_0 = -1$  at  $2\sigma$  CL.

- For the  $w$ CCCDM model, a significant portion of the  $w_0 - H_0$  parameter space indicates that the quintessence region ( $w_0 > -1$ ) is allowed within approximately  $1\sigma$ . In contrast, for the  $w$ CDM model, only a small quintessence region is permitted within  $2\sigma$ . We find that  $w_0 = -1$  can be well-accommodated in both the  $w$ CDM and  $w$ CCCDM models, though the parameter space that supports this is in tension with the SH0ES  $H_0$  value. Thus, with constant DE fluid parametrization one needs to move toward a phantom behaviour, to address the  $H_0$  tension, which is not an ideal framework for theoretical modelling.
- For the CPLCDM and CPLCCCDM models, the majority of the  $w_0 - H_0$  parameter space for shows  $w_0$  lies in the non-phantom region for the P18+DESI data combination. When subjected to the P18+DESI+PP+SH0ES data sets, the CPLCDM model shows that  $w_0$  always lies in the non-phantom region. In the case of the CPLCCCDM model, the majority of the  $w_0 - H_0$  parameter space lies in the non-phantom region (see extreme right panel of Fig. 2). Thus, dynamical fluid parametrization models are physically more viable compared to the constant dark energy fluid parameterizations.
- In Fig.3(a)-(c), we plot the  $w_0 - w_a$  parameter space for CPLCDM and CPLCCCDM models, showing similar behaviour for both cases studied. The constraints on the dark energy EoS parameter  $w_a$  for the CPLCCCDM model are slightly tighter compared to the conventional CPLCDM model as shown in Table. I.

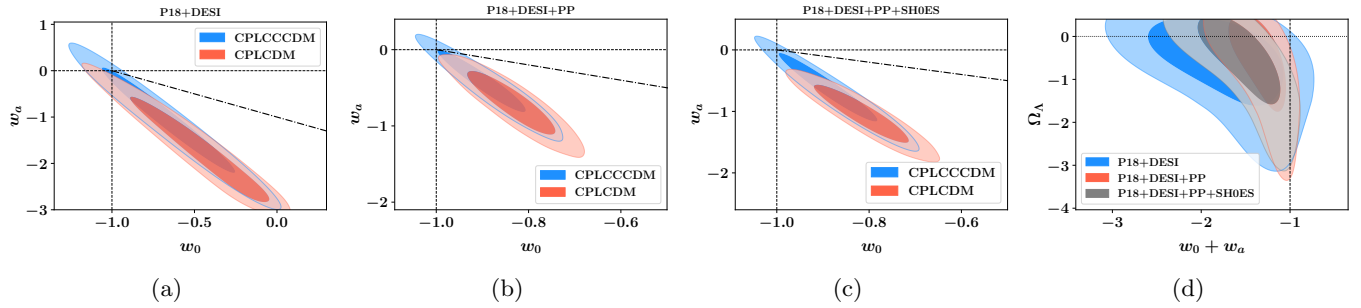


FIG. 3: 2D confidence contours at 68% and 95% confidence levels for  $w_0$  and  $w_a$ , to compare between CPLCDM and CPLCCDM with three dataset combinations: (a) P18+DESI, (b) P18+DESI+PP, (c) P18+DESI+PP+SH0ES respectively. (d) Plot for  $w_0 + w_a$  vs.  $\Omega_\Lambda$  for CPLCCDM, where  $\Omega_\Lambda = 0$  denotes CPLCDM.

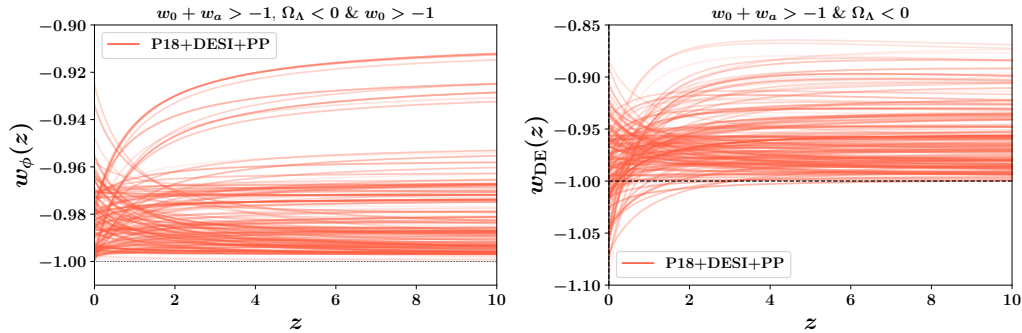


FIG. 4: Evolution of the total DE EoS  $w_{\text{DE}}(z)$ , along with the fluid's EoS,  $w_\phi(z)$  for the CPLCCDM model, derived from the P18+DESI+PP chains which satisfy the non-phantom behaviour at  $2\sigma$  CL.

8. We plot the contour for  $w_0 + w_a$  vs.  $\Omega_\Lambda$  in Fig. 3d. Here, the  $\Omega_\Lambda = 0$  line corresponds to the CPLCDM model, while the  $w_0 + w_a = -1$  line marks the phantom vs non-phantom divide. The results show that with the CPLCCDM model, regardless of the dataset combination, a small quintessence region is allowed within  $2\sigma$ , when the contribution from nCC to the DE sector is included.
9. The constrained mean values of  $\Omega_\Lambda$  are found to be negative, as shown in Table. I. For KiDS, a negative  $\Omega_\Lambda$  is well consistent at  $1\sigma$  CL for the  $w\text{CCCDM}$  model. In the CPLCCDM model,  $\Omega_\Lambda = 0$  is included within  $1\sigma$ . Similarly, for other data combinations,  $\Omega_\Lambda = 0$  remains within  $1\sigma$ , although the best-fit values consistently indicate a preference for  $\Omega_\Lambda < 0$ .
10. In Fig. 4, we present the evolution of the total dark energy EoS  $w_{\text{DE}}(z)$ , along with the fluid's EoS,  $w_\phi(z) \equiv w(z) = w_0 + w_a \left(\frac{z}{1+z}\right)$ , derived directly from the P18+DESI+PP MCMC chains for the CPLCCDM model which lies in the non-phantom region. The plot illustrates that the evolving part of the dark energy sector, which is contributed by the CPL/fluid parameterization of CPLCCDM, can strictly remain non-phantom under the conditions:  $w_0 + w_a > -1$ ,  $\Omega_\Lambda < 0$ , and  $w_0 > -1$ . However, the total dark en-

Model	KiDS		P18+DESI		P18+DESI+PP	
	$\Delta\chi^2$	$\Delta\ln(\mathcal{Z})$	$\Delta\chi^2$	$\Delta\ln(\mathcal{Z})$	$\Delta\chi^2$	$\Delta\ln(\mathcal{Z})$
$w\text{CCCDM}-w\text{CDM}$	-1.76	0.506	-0.051	-0.138	-0.946	-0.455
CPLCCDM-CPLCDM	-1.56	0.865	-0.108	-0.471	-0.989	-0.484

TABLE II: Model comparison:  $\Delta\chi^2 \equiv \chi_{\text{nCC}}^2 - \chi_{\text{no-nCC}}^2$ , and Bayesian Evidence  $\Delta\ln(\mathcal{Z}) \equiv \ln(\mathcal{Z})_{\text{nCC}} - \ln(\mathcal{Z})_{\text{no-nCC}}$ .

- ergy evolution can accommodate both phantom and non-phantom behaviour if the conditions  $w_0 + w_a > -1$  and  $\Omega_\Lambda < 0$  are imposed.
11. Table II highlights small changes in both  $\Delta\chi^2$  and  $\Delta\ln(\mathcal{Z})$ , with negative  $\Delta\chi^2$  across all datasets, suggesting that nCC models provide a slightly better fit than non-nCC models. The relative change in Bayesian evidence values is nearly negligible, indicating an almost indistinguishable difference between nCC and non-nCC models. We comment that, based on the current data, the nCC and non-nCC models are thus statistically indistinguishable and equally viable. Importantly, the inclusion of an AdS in the dark energy sector does not degrade the quality of the fit.
  12. The  $w_0 - w_a$  constraints from the CPLCDM model suggest that our universe transitions from an early-phantom to a late non-phantom phase, with a

phantom-to-non-phantom crossing at later times. Early phantom behaviour could lead to ghost instabilities due to the violation of the null energy condition (NEC) [51, 82]. The presence of an nCC contribution helps alleviate this strict early phantom nature, as a small region in the parameter space emerges that exhibits quintessence behaviour, which can be theoretically realized using scalar field models based on field theory, satisfying the NEC [71, 72].

Thus, incorporating an additional nCC component in the DE sector offers a significant advantage in modelling, as it enables a region in the  $w_0$ - $w_a$  parameter space that aligns with a non-phantom DE EoS. Moreover, a non-phantom behaviour can be physically well-motivated and is theoretically consistent, thereby facilitating more robust and reliable modelling of the DE sector.

This work investigates the role of a negative  $\Lambda$  in the DE sector, analyzing its implications using recent cosmological datasets, including P18, DESI, PP(+SH0ES) and KiDS. By comparing models with and without an nCC contribution ( $w$ CCCDM and CPLCCCDM vs  $w$ CDM and CPLCDM), we demonstrated that nCC models provide marginally better fits to the data, particularly when paired with the evolving DE  $w_0$   $w_a$ -parametrization. These models stand out for their ability to simultaneously resolve both the  $H_0$  and  $S_8$  tensions. The added advantage of the CPLCCCDM model, as shown in [62, 68] is that it can consistently explain the high- $z$ , massive, and bright galaxies observed by JWST, which the CPLCDM model fails to address. This underscores the robustness of the nCC framework in reconciling cosmological tensions, offering perspectives into hints for new physics, its potential origins and underlying mechanisms.

A key insight from our analysis is that the inclusion of nCC allows a quintessence behaviour throughout cosmic time without requiring strongly phantom values of the DE EoS. While the Bayesian evidence differences between nCC and non-nCC models are not decisive, the marginally improved fits to data, theoretical consistency, and ability to resolve key cosmological tensions make nCC models compelling candidates for further investigation. Finally, upcoming observational galaxy surveys such as Euclid [83], the Vera Rubin Observatory [84], and next-generation CMB [85, 86] and 21 cm experiments [87], will play a critical role in testing the predictions of nCC models [88]. These surveys are set to provide more precise constraints on the DE sector, presenting an opportunity to confirm or refute evidence for the presence of an additional nCC component in the DE sector in shaping cosmic expansion and structure formation. The connection between AdS vacuum and string theory further strengthens the theoretical appeal of this framework. String theory naturally accommodates nCC through its AdS vacuum structure, supported

by the AdS/CFT correspondence [89, 90]. This linkage underscores the potential of the nCC models to bridge cosmological observations with high-energy physics, paving the way for a more unified understanding of the universe.

PM acknowledges funding from the Anusandhan National Research Foundation (ANRF), Govt of India under the National Post-Doctoral Fellowship (File no. PDF/2023/001986). DK acknowledges the Ministry of Education (MoE) fellowship at MNIT Jaipur. AAS acknowledges the funding from ANRF, Govt of India under the research grant no. CRG/2023/003984. We acknowledge the use of the HPC facility, Pegasus, at IUCAA, Pune, India.

---

\* [pdf.p mukherjee@jmi.ac.in](mailto:pdf.p mukherjee@jmi.ac.in)

† [2019rpy9096@mmit.ac.in](mailto:2019rpy9096@mmit.ac.in)

‡ [aasen@jmi.ac.in](mailto:aasen@jmi.ac.in)

- [1] N. Aghanim *et al.* (Planck), *Astron. Astrophys.* **641**, A6 (2020), [Erratum: *Astron. Astrophys.* 652, C4 (2021)], [arXiv:1807.06209](https://arxiv.org/abs/1807.06209) [[astro-ph.CO](#)].
- [2] M. Tristram *et al.*, *Astron. Astrophys.* **682**, A37 (2024), [arXiv:2309.10034](https://arxiv.org/abs/2309.10034) [[astro-ph.CO](#)].
- [3] D. Brout *et al.*, *Astrophys. J.* **938**, 110 (2022), [arXiv:2202.04077](https://arxiv.org/abs/2202.04077) [[astro-ph.CO](#)].
- [4] T. M. C. Abbott *et al.* (DES), *Astrophys. J. Lett.* **973**, L14 (2024), [arXiv:2401.02929](https://arxiv.org/abs/2401.02929) [[astro-ph.CO](#)].
- [5] D. Rubin *et al.*, (2023), [arXiv:2311.12098](https://arxiv.org/abs/2311.12098) [[astro-ph.CO](#)].
- [6] S. Alam *et al.* (eBOSS), *Phys. Rev. D* **103**, 083533 (2021), [arXiv:2007.08991](https://arxiv.org/abs/2007.08991) [[astro-ph.CO](#)].
- [7] A. G. Adame *et al.* (DESI), (2024), [arXiv:2411.12021](https://arxiv.org/abs/2411.12021) [[astro-ph.CO](#)].
- [8] A. G. Adame *et al.* (DESI), (2024), [arXiv:2404.03001](https://arxiv.org/abs/2404.03001) [[astro-ph.CO](#)].
- [9] A. G. Adame *et al.* (DESI), (2024), [arXiv:2404.03000](https://arxiv.org/abs/2404.03000) [[astro-ph.CO](#)].
- [10] Y. B. Zel'dovich, A. Krasinski, and Y. B. Zel'dovich, *Sov. Phys. Usp.* **11**, 381 (1968).
- [11] S. Weinberg, *Rev. Mod. Phys.* **61**, 1 (1989).
- [12] V. Sahni and A. A. Starobinsky, *Int. J. Mod. Phys. D* **9**, 373 (2000), [arXiv:astro-ph/9904398](https://arxiv.org/abs/astro-ph/9904398).
- [13] D. K. Hazra, S. Majumdar, S. Pal, S. Panda, and A. A. Sen, *Phys. Rev. D* **91**, 083005 (2015), [arXiv:1310.6161](https://arxiv.org/abs/1310.6161) [[astro-ph.CO](#)].
- [14] L. Verde, T. Treu, and A. G. Riess, *Nature Astron.* **3**, 891 (2019), [arXiv:1907.10625](https://arxiv.org/abs/1907.10625) [[astro-ph.CO](#)].
- [15] A. G. Riess *et al.*, *Astrophys. J. Lett.* **934**, L7 (2022), [arXiv:2112.04510](https://arxiv.org/abs/2112.04510) [[astro-ph.CO](#)].
- [16] E. Di Valentino *et al.*, *Astropart. Phys.* **131**, 102605 (2021), [arXiv:2008.11284](https://arxiv.org/abs/2008.11284) [[astro-ph.CO](#)].
- [17] E. Di Valentino *et al.*, *Astropart. Phys.* **131**, 102604 (2021), [arXiv:2008.11285](https://arxiv.org/abs/2008.11285) [[astro-ph.CO](#)].
- [18] T. M. C. Abbott *et al.* (DES), *Phys. Rev. D* **105**, 023520 (2022), [arXiv:2105.13549](https://arxiv.org/abs/2105.13549) [[astro-ph.CO](#)].
- [19] C. Heymans *et al.*, *Astron. Astrophys.* **646**, A140 (2021), [arXiv:2007.15632](https://arxiv.org/abs/2007.15632) [[astro-ph.CO](#)].

- [20] X. Li *et al.*, *Phys. Rev. D* **108**, 123518 (2023), [arXiv:2304.00702 \[astro-ph.CO\]](#).
- [21] I. Labbe *et al.*, *Nature* **616**, 266 (2023), [arXiv:2207.12446 \[astro-ph.GA\]](#).
- [22] M. Boylan-Kolchin, *Nature Astron.* **7**, 731 (2023), [arXiv:2208.01611 \[astro-ph.CO\]](#).
- [23] E. Di Valentino, O. Mena, S. Pan, L. Visinelli, W. Yang, A. Melchiorri, D. F. Mota, A. G. Riess, and J. Silk, *Class. Quant. Grav.* **38**, 153001 (2021), [arXiv:2103.01183 \[astro-ph.CO\]](#).
- [24] L. Perivolaropoulos and F. Skara, *New Astron. Rev.* **95**, 101659 (2022), [arXiv:2105.05208 \[astro-ph.CO\]](#).
- [25] E. Abdalla *et al.*, *JHEAp* **34**, 49 (2022), [arXiv:2203.06142 \[astro-ph.CO\]](#).
- [26] V. Sahni and A. Starobinsky, *Int. J. Mod. Phys. D* **15**, 2105 (2006), [arXiv:astro-ph/0610026](#).
- [27] D. Huterer and D. L. Shafer, *Rept. Prog. Phys.* **81**, 016901 (2018), [arXiv:1709.01091 \[astro-ph.CO\]](#).
- [28] A. G. Adame *et al.* (DESI), (2024), [arXiv:2404.03002 \[astro-ph.CO\]](#).
- [29] A. G. Adame *et al.* (DESI), (2024), [arXiv:2411.12022 \[astro-ph.CO\]](#).
- [30] K. Lodha *et al.* (DESI), *Phys. Rev. D* **111**, 023532 (2025), [arXiv:2405.13588 \[astro-ph.CO\]](#).
- [31] M. Cortés and A. R. Liddle, *JCAP* **12**, 007 (2024), [arXiv:2404.08056 \[astro-ph.CO\]](#).
- [32] C.-G. Park, J. de Cruz Pérez, and B. Ratra, *Phys. Rev. D* **110**, 123533 (2024), [arXiv:2405.00502 \[astro-ph.CO\]](#).
- [33] W. J. Wolf and P. G. Ferreira, *Phys. Rev. D* **108**, 103519 (2023), [arXiv:2310.07482 \[astro-ph.CO\]](#).
- [34] I. D. Gialamas, G. Hütsi, K. Kannike, A. Racioppi, M. Raidal, M. Vasar, and H. Veermäe, (2024), [arXiv:2406.07533 \[astro-ph.CO\]](#).
- [35] J.-Q. Jiang, D. Pedrotti, S. S. da Costa, and S. Vagnozzi, *Phys. Rev. D* **110**, 123519 (2024), [arXiv:2408.02365 \[astro-ph.CO\]](#).
- [36] B. R. Dinda, *JCAP* **09**, 062 (2024), [arXiv:2405.06618 \[astro-ph.CO\]](#).
- [37] D. Wang, (2024), [arXiv:2404.06796 \[astro-ph.CO\]](#).
- [38] E. O. Colgáin, M. G. Dainotti, S. Capozziello, S. Pourojaghi, M. M. Sheikh-Jabbari, and D. Stojkovic, (2024), [arXiv:2404.08633 \[astro-ph.CO\]](#).
- [39] S. Bhattacharya, G. Borghetto, A. Malhotra, S. Parameswaran, G. Tasinato, and I. Zavala, *JCAP* **09**, 073 (2024), [arXiv:2405.17396 \[astro-ph.CO\]](#).
- [40] A. G. Ferrari, M. Ballardini, F. Finelli, and D. Paoletti, (2025), [arXiv:2501.15298 \[astro-ph.CO\]](#).
- [41] C.-G. Park and B. Ratra, (2025), [arXiv:2501.03480 \[astro-ph.CO\]](#).
- [42] W. J. Wolf, P. G. Ferreira, and C. García-García, (2024), [arXiv:2409.17019 \[astro-ph.CO\]](#).
- [43] B. Ghosh and C. Bengaly, *Phys. Dark Univ.* **46**, 101699 (2024), [arXiv:2408.04432 \[astro-ph.CO\]](#).
- [44] G. Ye, M. Martinelli, B. Hu, and A. Silvestri, (2024), [arXiv:2407.15832 \[astro-ph.CO\]](#).
- [45] R. Shah, P. Mukherjee, S. Saha, U. Garain, and S. Pal, (2024), [arXiv:2412.14750 \[astro-ph.CO\]](#).
- [46] P. Mukherjee and A. A. Sen, *Phys. Rev. D* **110**, 123502 (2024), [arXiv:2405.19178 \[astro-ph.CO\]](#).
- [47] Y. Tiwari, U. Upadhyay, and R. K. Jain, (2024), [arXiv:2412.00931 \[astro-ph.CO\]](#).
- [48] P. Mukherjee and A. A. Sen, (2024), [arXiv:2412.13973 \[astro-ph.CO\]](#).
- [49] R. Cardenas, T. Gonzalez, Y. Leiva, O. Martin, and I. Quiros, *Phys. Rev. D* **67**, 083501 (2003), [arXiv:astro-ph/0206315](#).
- [50] K. Dutta, Ruchika, A. Roy, A. A. Sen, and M. M. Sheikh-Jabbari, *Gen. Rel. Grav.* **52**, 15 (2020), [arXiv:1808.06623 \[astro-ph.CO\]](#).
- [51] C. Vafa, (2005), [arXiv:hep-th/0509212](#).
- [52] U. H. Danielsson and T. Van Riet, *Int. J. Mod. Phys. D* **27**, 1830007 (2018), [arXiv:1804.01120 \[hep-th\]](#).
- [53] G. Obied, H. Ooguri, L. Spodyneiko, and C. Vafa, (2018), [arXiv:1806.08362 \[hep-th\]](#).
- [54] S. K. Garg and C. Krishnan, *JHEP* **11**, 075 (2019), [arXiv:1807.05193 \[hep-th\]](#).
- [55] M. Cicoli, S. De Alwis, A. Maharana, F. Muia, and F. Quevedo, *Fortsch. Phys.* **67**, 1800079 (2019), [arXiv:1808.08967 \[hep-th\]](#).
- [56] J. M. Maldacena, *Adv. Theor. Math. Phys.* **2**, 231 (1998), [arXiv:hep-th/9711200](#).
- [57] O. Akarsu, J. D. Barrow, L. A. Escamilla, and J. A. Vazquez, *Phys. Rev. D* **101**, 063528 (2020), [arXiv:1912.08751 \[astro-ph.CO\]](#).
- [58] L. Visinelli, S. Vagnozzi, and U. Danielsson, *Symmetry* **11**, 1035 (2019), [arXiv:1907.07953 \[astro-ph.CO\]](#).
- [59] R. Calderón, R. Gannouji, B. L’Huillier, and D. Polarski, *Phys. Rev. D* **103**, 023526 (2021), [arXiv:2008.10237 \[astro-ph.CO\]](#).
- [60] A. A. Sen, S. A. Adil, and S. Sen, *Mon. Not. Roy. Astron. Soc.* **518**, 1098 (2022), [arXiv:2112.10641 \[astro-ph.CO\]](#).
- [61] G. Ye and Y.-S. Piao, *Phys. Rev. D* **101**, 083507 (2020), [arXiv:2001.02451 \[astro-ph.CO\]](#).
- [62] N. Menci, S. A. Adil, U. Mukhopadhyay, A. A. Sen, and S. Vagnozzi, *JCAP* **07**, 072 (2024), [arXiv:2401.12659 \[astro-ph.CO\]](#).
- [63] A. Gómez-Valent, A. Favale, M. Migliaccio, and A. A. Sen, *Phys. Rev. D* **109**, 023525 (2024), [arXiv:2309.07795 \[astro-ph.CO\]](#).
- [64] Ruchika, S. A. Adil, K. Dutta, A. Mukherjee, and A. A. Sen, *Phys. Dark Univ.* **40**, 101199 (2023), [arXiv:2005.08813 \[astro-ph.CO\]](#).
- [65] J.-Q. Jiang and Y.-S. Piao, *Phys. Rev. D* **104**, 103524 (2021), [arXiv:2107.07128 \[astro-ph.CO\]](#).
- [66] S. A. Adil, O. Akarsu, E. Di Valentino, R. C. Nunes, E. Özüiker, A. A. Sen, and E. Specogna, *Phys. Rev. D* **109**, 023527 (2024), [arXiv:2306.08046 \[astro-ph.CO\]](#).
- [67] H. Wang, Z.-Y. Peng, and Y.-S. Piao, (2024), [arXiv:2406.03395 \[astro-ph.CO\]](#).
- [68] N. Menci, A. A. Sen, and M. Castellano, *Astrophys. J.* **976**, 227 (2024), [arXiv:2410.22940 \[astro-ph.CO\]](#).
- [69] M. Chevallier and D. Polarski, *Int. J. Mod. Phys. D* **10**, 213 (2001), [arXiv:gr-qc/0009008](#).
- [70] E. V. Linder, *Phys. Rev. Lett.* **90**, 091301 (2003), [arXiv:astro-ph/0208512](#).
- [71] B. Ratra and P. J. E. Peebles, *Phys. Rev. D* **37**, 3406 (1988).
- [72] R. R. Caldwell, R. Dave, and P. J. Steinhardt, *Phys. Rev. Lett.* **80**, 1582 (1998), [arXiv:astro-ph/9708069](#).
- [73] M. Asgari *et al.* (KiDS), *Astron. Astrophys.* **645**, A104 (2021), [arXiv:2007.15633 \[astro-ph.CO\]](#).
- [74] P. Schneider, T. Eifler, and E. Krause, *Astronomy and Astrophysics* **520**, A116 (2010).
- [75] D. Blas, J. Lesgourgues, and T. Tram, *JCAP* **07**, 034 (2011), [arXiv:1104.2933 \[astro-ph.CO\]](#).
- [76] B. Audren, J. Lesgourgues, K. Benabed, and S. Prunet, *JCAP* **1302**, 001 (2013), [arXiv:1210.7183 \[astro-ph.CO\]](#).

- [77] T. Brinckmann and J. Lesgourgues, (2018), [arXiv:1804.07261 \[astro-ph.CO\]](#).
- [78] J. Torrado and A. Lewis, *JCAP* **05**, 057 (2021), [arXiv:2005.05290 \[astro-ph.IM\]](#).
- [79] A. Lewis, (2019), [arXiv:1910.13970 \[astro-ph.IM\]](#).
- [80] F. Feroz, M. P. Hobson, and M. Bridges, *Mon. Not. Roy. Astron. Soc.* **398**, 1601 (2009), [arXiv:0809.3437 \[astro-ph\]](#).
- [81] F. Feroz, M. P. Hobson, E. Cameron, and A. N. Pettitt, *Open J. Astrophys.* **2**, 10 (2019), [arXiv:1306.2144 \[astro-ph.IM\]](#).
- [82] I. Y. Aref'eva and I. V. Volovich, *Theor. Math. Phys.* **155**, 503 (2008), [arXiv:hep-th/0612098](#).
- [83] L. Amendola *et al.*, *Living Rev. Rel.* **21**, 2 (2018), [arXiv:1606.00180 \[astro-ph.CO\]](#).
- [84] B. Blum *et al.*, in *Snowmass 2021* (2022) [arXiv:2203.07220 \[astro-ph.CO\]](#).
- [85] M. Hazumi *et al.* (LiteBIRD), *Proc. SPIE Int. Soc. Opt. Eng.* **11443**, 114432F (2020), [arXiv:2101.12449 \[astro-ph.IM\]](#).
- [86] K. N. Abazajian *et al.* (CMB-S4), (2016), [arXiv:1610.02743 \[astro-ph.CO\]](#).
- [87] R. Dutta *et al.*, *J. Astrophys. Astron.* **43**, 103 (2022), [arXiv:2209.09264 \[astro-ph.GA\]](#).
- [88] C. B. V. Dash, T. G. Sarkar, and A. A. Sen, *Mon. Not. Roy. Astron. Soc.* **527**, 11694 (2023), [arXiv:2309.01623 \[astro-ph.CO\]](#).
- [89] M. Demirtas, M. Kim, L. McAllister, J. Moritz, and A. Rios-Tascon, *Phys. Rev. Lett.* **128**, 011602 (2022), [arXiv:2107.09065 \[hep-th\]](#).
- [90] M. Van Raamsdonk and C. Waddell, *JCAP* **06**, 047 (2024), [arXiv:2305.04946 \[astro-ph.CO\]](#).